

Bubble wall correlations in cosmological phase transitions

Ariel Mégevand* and Federico Agustín Membiela†

IFIMAR (CONICET-UNMdP)

*Departamento de Física, Facultad de Ciencias Exactas y Naturales,
UNMdP, Deán Funes 3350, (7600) Mar del Plata, Argentina*

Abstract

We study statistical relationships between bubble walls in cosmological first-order phase transitions. We consider the conditional and joint probabilities for different points on the walls to remain uncollided at given times. We use these results to discuss surface correlations which are relevant for the consequences of the transition. In our statistical treatment, the kinematics of bubble nucleation and growth is characterized by the nucleation rate and the wall velocity as functions of time, and we obtain general expressions in terms of these two quantities. As a specific example, we consider a model with simultaneous nucleation and constant velocity.

1 Introduction

It is well known that first-order phase transitions may have occurred in the early universe, and may have left several potentially observable remnants. In a cosmological first-order phase transition, a metastable high-temperature phase (false vacuum) undergoes supercooling, and then the phase transition proceeds through the nucleation and expansion of bubbles of the low-temperature stable phase (true vacuum). The dynamics is different in the case of a “vacuum” transition and in the case of a “thermal” transition [1, 2]. In the former case, the nucleation of bubbles occurs in the absence of a plasma, and the nucleation rate Γ is given by the probability of decay of the false vacuum per unit time per unit volume [3, 4]. Besides, all the false-vacuum energy, which is released at the bubble walls, goes into accelerating the latter, which reach velocities $v \simeq 1$. This may also occur in a thermal phase transition with extreme supercooling, in which the wall velocity may exhibit runaway behavior [5, 6]. The bubble walls disappear as bubbles collide, and the energy stored in the walls is transferred to thermal energy. On the other hand, a thermal transition occurs in the presence of a plasma, and we have a temperature-dependent nucleation rate $\Gamma(T)$ [7, 8]. In this case, the walls generally reach a terminal velocity $v(T)$,

*Member of CONICET, Argentina. E-mail address: megevand@mdp.edu.ar

†Member of CONICET, Argentina. E-mail address: membiela@mdp.edu.ar

and most of the released energy (latent heat) goes to the fluid. Therefore, as the walls move, a reheating of the plasma occurs, as well as bulk fluid motions.

Even in the thin wall approximation, which is generally valid, the dynamics of thermal phase transitions is complex. In the first place, the nucleation rate is very sensitive to temperature variations. In the second place, the wall velocity depends on the microphysics which determines the friction with the plasma [9, 10], and is also affected by the hydrodynamics [11, 12, 13]. Nevertheless, in many cases it is possible to assume that the nucleation rate is homogeneous and that the bubbles are spherical and all expand with the same speed. In such cases, the bubble kinematics is determined by the two basic ingredients $\Gamma(t)$ and $v(t)$. The kinematics is also affected, to a greater or lesser extent, by the scale factor $a(t)$. In most cases, however, the variation of the latter can be neglected for the duration of the phase transition. An exception is the case of strongly-supercooled phase transitions [1, 14, 15]. In the statistical treatment of the phase transition, the quantities are averaged over possible realizations, and we shall denote $\langle Q \rangle$ the ensemble average of a quantity Q . In practice, these averages are calculated from the average number of bubbles nucleated in a given volume during a certain time, which is given by $\Gamma(t)$.

In the development of the transition, the most evident measure of progress is the volume fraction occupied by bubbles, $f_b(t)$. However, other quantities can be used as well, such as the fraction of bubble wall which remains uncollided, $f_S(t)$ [1]. Since the collided walls quickly¹ disappear inside merged bubbles², the uncollided wall area is essentially the total area S_{tot} that is physically present at time t . We have $S_{\text{tot}} = \sum_i S_i$, where S_i is the wall area of bubble i which remains (uncollided) at time t . The fraction of surface f_S is defined as S_{tot} divided by the total area $\sum_i 4\pi R_i^2$ of bubbles of radii R_i , including area that has been covered by bubbles. This quantity varies from $f_S = 1$ at the beginning of the phase transition (when bubbles are isolated) to $f_S = 0$ at the end (when all bubbles have merged and their walls have disappeared). The quantity f_S tracks the conversion of potential energy (false vacuum energy or latent heat) to other forms of energy (kinetic energy of the wall, kinetic energy of the fluid, or thermal energy). It will be more relevant than f_b to those processes involving the bubble walls. In particular, the departures from equilibrium which give rise to the important consequences of the phase transition originate at the bubble walls. Let us consider a few examples.

Baryogenesis. If the electroweak phase transition is of first order, the walls of expanding bubbles push a net charge density into the symmetric phase, which bias baryon-number violating processes [17, 18, 19, 20]. This mechanism relies on diffusion processes that take place up to a distance l from the wall, which is naturally $l \sim T^{-1}$. This length is several orders of magnitude smaller than the typical bubble radius R , which is of order H^{-1} , where H is the Hubble rate. It is in this very thin shell next to the bubble walls where baryon number generation occurs. The baryon number density $n_B(t)$ which is left behind by the walls depends on the value of the wall velocity. The latter is often estimated at

¹In general, all the terms in the equation of motion for the scalar field (order parameter) involve a single scale, namely, the scale of the theory, which is $\sim T$, so the characteristic time scale for the wall dynamics is $\sim T^{-1}$. This time is generally much shorter than the duration of the phase transition, which is determined by the Hubble rate and involves also the Planck scale.

²For recent discussions on the behavior of the scalar field after bubble collisions, see [16] and references therein.

the onset of nucleation, although $v(t)$ generally varies during the phase transition.

Gravitational waves. The energy that is set in motion by the bubble walls is a source of gravitational waves (GWs) [21, 22, 23]. This energy may be concentrated in the walls themselves, or it may be transferred to bulk fluid motions [24, 2]. In the latter case, the relation of the wall surface with the generated GW spectrum is indirect, since the direct source of GWs is the turbulence [2] or the sound waves [25] caused in the fluid, which may last longer than the phase transition. In any case, the walls are the source of such fluid motions. Furthermore, in the so called bubble-collision mechanism the energy transferred to the fluid is assumed to be concentrated in a thin shell around the walls. In the envelope approximation [26], the contribution of the overlap regions to the gravitational radiation is neglected, and the energy-momentum tensor is concentrated in the “envelope” of walls surrounding a cluster of bubbles.

Topological defects. Perhaps the simplest example illustrating the formation of topological defects [27] is the trapping of a vortex in two spatial dimensions. Consider the spontaneous symmetry-breaking of a global $U(1)$ symmetry, where a complex scalar field ϕ vanishes in the symmetric phase and takes nonvanishing values $\phi = ve^{i\alpha}$ in the broken-symmetry phase. The modulus v is fixed but the phase α is arbitrary and is uncorrelated in different bubbles. When two bubbles meet, α will rearrange itself so that it varies smoothly from one bubble to the other. Moreover, this phase will tend to take a constant value throughout space. When three bubbles meet at a given point, α will tend to vary smoothly along a closed line across the three bubbles. However, a complete equilibration to reach a constant phase may be topologically impossible, in which case a defect will be trapped in a symmetric-phase region enclosed by the bubbles. Nevertheless, it is very unlikely that three bubble walls collide simultaneously at a single point. Two of the bubbles will meet first, and the third one will arrive later. If the phase equilibration [28] between the first two bubbles completes before the arrival of the third bubble, the formation of a vortex may be avoided [29].

It is clear that the wall dynamics plays a relevant role in the determination of these consequences of the phase transition. In particular, electroweak baryogenesis takes place in a thin shell next to the bubble walls. Since the baryon number density depends on the wall velocity, a precise evaluation of the baryon asymmetry requires integrating $n_B(t)$ in time, weighted with the volume $\langle S_{\text{tot}}(t) \rangle v(t) dt$. In the case of GW production (at least in the envelope approximation), the energy-momentum tensor T is also localized in a thin shell around the bubble walls. However, the spectrum of GWs depends on the correlation function $\langle T(x)T(y) \rangle$ between different space-time points (see, e.g., [30, 31]). One would then expect that the GW spectrum will be related to bubble surface correlations $\langle S(t)S(t') \rangle$ rather than to the average area. On the other hand, for topological defect formation, the probability of trapping a defect in a sequence of bubble collisions depends on the probability that a point on a given bubble wall will soon collide once a nearby point has already collided. This mechanism should then be related to the correlation between different points on the same bubble wall.

It is well known that the probability that a random point of space is in the false vacuum is the same as the fraction of volume remaining in that phase. Also, the fraction of the bubble wall that remains uncollided is given by the probability that a point *on a*

bubble wall remains in the false vacuum (this probability is not the same as the previous one, since the nucleation in the vicinity of the point is affected by the presence of the bubble to which it belongs [1]). Similarly, the surface correlations mentioned above will depend on conditional or joint probabilities for multiple points belonging to bubble walls.

In the present paper, we consider such probabilities. In the next section we review some existing results and discuss the probability that a set of arbitrary points in space remain in the false vacuum at a given time. In section 3 we calculate the probability that a point in the surface of a bubble is uncollided, depending on whether another point in the same bubble wall or in the wall of another bubble is still uncollided. In section 4 we consider some applications, such as wall area correlations. We apply the results to a specific model for the phase transition, in which bubbles nucleate simultaneously and the wall velocity is constant. We finish with a discussion in section 5.

2 Phase transition dynamics and probability of remaining in the false vacuum

In this section and the following we shall consider the dynamics of the phase transition for arbitrary $\Gamma(t)$ and $v(t)$, while in section 4 we shall consider a particular example. Actually, rather than the wall velocity, the basic ingredient will be the bubble radius. Between two times t' and t , the radius of a bubble increases by

$$R(t', t) = \int_{t'}^t v(t'') dt''. \quad (1)$$

For simplicity, we shall ignore the effect of the scale factor $a(t)$, which would introduce a factor $a(t)/a(t')$ in the integrand. As already mentioned, this approximation is valid in most cases. In any case, generalizing our treatment to include this effect should be straightforward. If we neglect the initial radius of the bubble at the time of its nucleation, which is also a good approximation in general, then Eq. (1) gives the radius of a bubble which has nucleated at time t' and has expanded until time t . The fraction of volume occupied by bubbles is given by $f_b = 1 - P_{fv}$, where P_{fv} is the fraction of volume in the false vacuum, which coincides with the probability that an arbitrary point is in that phase. This quantity is well known [32]. We shall consider a derivation here, which we shall generalize to less simple cases below.

2.1 Probability that a given point in space remains in the false vacuum

By time t , a point p may have been reached by bubbles nucleated at times $t'' < t$. We begin by considering the probability $P_{\text{out}}(t'')$ that p , at time t , is outside of any bubbles nucleated before a certain t'' . This probability depends also on t , which we omit for simplicity of notation. Then, the probability that p remains outside of any bubbles nucleated before $t'' + dt''$ is given by the product

$$P_{\text{out}}(t'' + dt'') = P_{\text{out}}(t'')(1 - dP(t'')), \quad (2)$$

where the last factor is the probability that p was not reached by bubbles nucleated between t'' and $t'' + dt''$ either. That is to say, $dP(t'')$ is the probability that p has been

reached by some bubble nucleated between t'' and $t'' + dt''$, assuming that p was not reached by bubbles nucleated before t'' . From Eq. (2) we readily obtain a differential equation whose solution is

$$P_{\text{out}}(t'') = e^{-\int_{t_c}^{t''} dP}. \quad (3)$$

Here, t_c is the initial time, corresponding to the critical temperature T_c of the phase transition, before which the nucleation rate vanishes. Evaluating at $t'' = t$ we obtain the probability that the point p remains in the false vacuum at time t ,

$$P_{fv}(t) = e^{-\int_{t_c}^t dP(t'')}. \quad (4)$$

We still have to compute the conditional probability $dP(t'')$ that (at time t) p is inside a bubble nucleated between t'' and $t'' + dt''$, assuming that it is outside of any previously nucleated bubbles. For a bubble nucleated at time t'' to reach the point p before time t , the bubble must have nucleated at a distance smaller than $R(t'', t)$ from the point. In Fig. 1, the dots represent the possible nucleation points. To calculate the probability that a bubble was nucleated within this radius at time t'' , we must determine whether, at that time, the whole region was actually available for bubble nucleation, since part of the space could have been occupied by previously nucleated bubbles. Nevertheless, such bubbles would also reach the point p before time t , which we are assuming does not occur. Indeed, consider a bubble nucleated at a certain $t_{\text{prev}} < t''$. For this bubble to invade the dotted region at t'' , it must have nucleated at a distance smaller than $R(t_{\text{prev}}, t'')$ from it (see Fig. 1). But then it would be too close to p , at a distance smaller than $R(t_{\text{prev}}, t'') + R(t'', t) = R(t_{\text{prev}}, t)$.

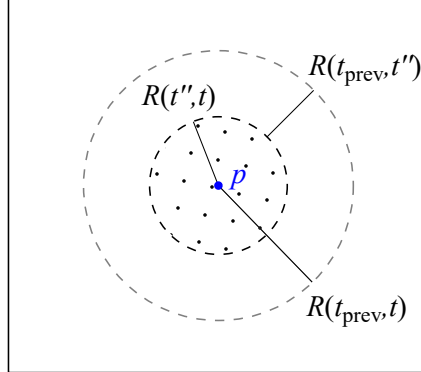


Figure 1: The region in which bubbles must nucleate at time t'' in order to reach the point p before time t (dots). The outer circle indicates the region within which bubbles should nucleate at $t_{\text{prev}} < t''$ in order to affect the dotted region.

Hence, the whole volume of the dotted region is free of bubbles at time t'' and is available for nucleations. Thus, the probability $dP(t'')$ is given by

$$dP(t'') = dt'' \Gamma(t'') \frac{4\pi}{3} R(t'', t)^3. \quad (5)$$

From (4-5) we obtain

$$P_{fv}(t) = e^{-I(t)}, \quad (6)$$

where

$$I(t) = \int_{t_c}^t dt'' \Gamma(t'') \frac{4\pi}{3} R(t'', t)^3. \quad (7)$$

2.2 Probability that a point is in the false vacuum given that another point is in the false vacuum

Let us now consider the probability $P_{p|p'}$ that a point p remains in the false vacuum at time t , given that another point p' was in the false vacuum at time $t' \leq t$. Proceeding as before, we consider the probability $P_{\text{out}}(t'')$ that p has not been reached by bubbles nucleated before t'' , and then the probability $dP(t'')$ that p has been reached by a bubble nucleated between t'' and $t'' + dt''$. Thus, we obtain the same equation for $P_{\text{out}}(t'')$, Eq. (2), which leads to Eqs. (3) and (4). Like in the previous case, $dP(t'')$ is the conditional probability that p is inside a bubble nucleated between t'' and $t'' + dt''$ subjected to the condition that p is outside of bubbles nucleated before t'' . The difference is that, in the present case, we also have the condition that the other point, p' , is in the false vacuum at time t' . Therefore, we write

$$P_{p|p'} = e^{-\int_{t_c}^t dP(t'')}, \quad (8)$$

and we must re-evaluate the conditional probability $dP(t'')$.

At t'' , the bubble affecting p must have nucleated within a sphere of radius $R(t'', t)$ centered at this point, like in Fig. 1. Then, in principle, we would obtain Eq. (5). Again, under the present conditions the dotted region is not affected, at time t'' , by previously nucleated bubbles. However, the nucleations at t'' might reach the point p' before time t' , which is now forbidden by the conditional probability. For $t'' > t'$ this will not happen, so we still have

$$dP(t'') = dt'' \Gamma(t'') \frac{4\pi}{3} R(t'', t)^3 \quad (t'' > t'). \quad (9)$$

But for $t'' \leq t'$, any nucleation at time t'' must occur at a distance larger than $R(t'', t')$ from p' in order to avoid affecting this point. This situation is represented in Fig. 2. A nucleation at t'' must occur inside the dotted region in order to affect the point p but outside the striped region to leave p' unaffected. Therefore, we have

$$dP(t'') = dt'' \Gamma(t'') \left[\frac{4\pi}{3} R(t'', t)^3 - V_{\cap} \right] \quad (t'' \leq t'), \quad (10)$$

where V_{\cap} is the volume of the intersection of the two spheres.

From Eqs. (8-10), we obtain

$$P_{p|p'} = \exp \left[- \int_{t_c}^t dt'' \Gamma(t'') \frac{4\pi}{3} R(t'', t)^3 + \int_{t_c}^{t'} dt'' \Gamma(t'') V_{\cap} \right]. \quad (11)$$

The intersection volume V_{\cap} depends on the radii

$$r \equiv R(t'', t), \quad r' \equiv R(t'', t') \quad (12)$$

and on the separation s between p and p' . It is given by

$$V_{\cap} = \begin{cases} 4\pi r'^3/3 & \text{for } s \leq r - r', \\ \frac{\pi}{12}(r + r' - s)^2 \left[s + 2(r + r') - \frac{3(r-r')^2}{s} \right] & \text{for } r - r' < s \leq r + r', \\ 0 & \text{for } s > r + r'. \end{cases} \quad (13)$$

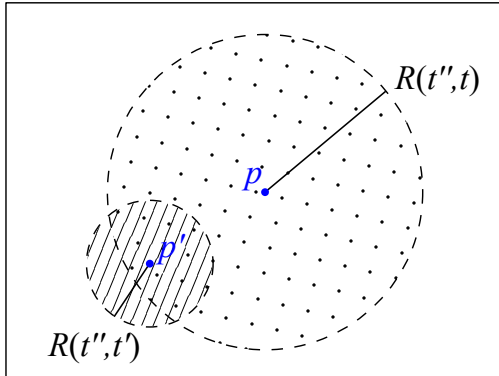


Figure 2: Regions affecting the points p and p' for $t'' < t' < t$. The dotted region is that in which a bubble must nucleate at time t'' in order to reach the point p before time t . If the nucleation occurs inside the striped region, the bubble would eat the point p' before time t' .

Notice that, if the separation is small enough, the smaller sphere is completely contained inside the larger one³; hence the value $4\pi r'^3/3$. On the other hand, if the separation is large enough, the intersection is empty and we have $V_{\cap} = 0$ (see Fig. 2). Finally, we write Eq. (11) in the form

$$P_{p|p'}(t, t', s) = \exp[-I(t) + I_{\cap}(t, t', s)], \quad (14)$$

where the function $I(t)$ is given by Eq. (7), and we have defined the quantity

$$I_{\cap}(t, t', s) = \int_{t_c}^{t'} dt'' \Gamma(t'') V_{\cap}(r, r', s). \quad (15)$$

2.3 Probability that multiple points remain in the false vacuum

Although we are mostly interested in points on bubble walls, we shall comment on the probability for several arbitrary points to remain in the false vacuum. We have obtained the probability $P_{p|p'}(t, t', s)$ of the point p being in the false vacuum at time t , under the condition that p' was in the false vacuum at time $t' \leq t$. Multiplying by the probability $P_{fv}(t')$ that p' was in the false vacuum at time t' , Eq. (6), we obtain the joint probability⁴ that p is in the false vacuum at time t and p' is in the false vacuum at time t' ,

$$P_{fv}^{(2)}(t, t', s) = P_{fv}(t') P_{p|p'}(t, t', s) = \exp[-I(t) - I(t') + I_{\cap}(t, t', s)] \quad (16)$$

(we denote the two-point case with a superscript 2). The exponent in the last expression can be written as $-I_{\cup}$, with

$$I_{\cup}(t, t', s) = \int_{t_c}^t dt'' \Gamma(t'') V_{\cup}, \quad (17)$$

³Remember that we are considering the specific case $t' \leq t$, so we have $r' \leq r$. For $t' > t$ (in which case the probability $P_{p|p'}$ is conditioned to the point p' being in the false vacuum in the future) the calculation is similar, and the result is essentially the same. To take into account this possibility, the limit of integration t' in the second integral of Eq. (11) must be replaced with $t_m = \min\{t, t'\}$.

⁴For this joint probability, there is no loss of generality in the assumption $t' \leq t$.

where V_{\cup} is the volume of the union of the two spheres of radii $R(t'', t)$ and $R(t'', t')$,

$$V_{\cup} = \frac{4\pi}{3}r^3 + \left[\frac{4\pi}{3}r'^3 + V_{\cap}(r, r', s) \right] \Theta(t' - t''). \quad (18)$$

This expression takes into account the fact that there is no sphere of radius $R(t'', t')$ for $t'' > t'$.

We could have obtained this result⁵ as a generalization of the calculation of $P_{fv}^{(1)}(t) \equiv P_{fv}(t)$. In this case, $P_{\text{out}}(t'')$ would denote the probability that *none* of the two points p, p' has been eaten by bubbles nucleated before time t'' , and $dP(t'')$ the probability that *at least one* of them has been reached by a bubble nucleated between t'' and $t'' + dt''$. This leads to the total volume V_{\cup} . The generalization to the probability that n points p_1, \dots, p_n remain in the false vacuum at times t_1, \dots, t_n , respectively, is straightforward. For a bubble nucleated at time t'' to reach any of the points p_i before the corresponding time t_i , the bubble must have nucleated within one of the spheres of radius $R(t'', t_i)$ centered at p_i . This is illustrated in Fig. 3 for the case of three points. The result involves the volume V_{\cup} of the union of the n spheres, which depends on the separations s_{ij} between the different points p_i as well as on the radii $R(t'', t_i)$. Thus, we have

$$P_{fv}^{(n)}(t_i, s_{ij}) = e^{-I_{\cup}(t_i, s_{ij})}, \quad (19)$$

where $I_{\cup} = \int_{t_c}^{t_{\max}} dt'' \Gamma(t'') V_{\cup}$ and $t_{\max} = \max\{t_i\}$. The computation of V_{\cup} must take into account that for $t'' > t_i$ we have $R(t'', t_i) = 0$. Care must also be taken of avoiding over-counting the intersections, which may be multiple.

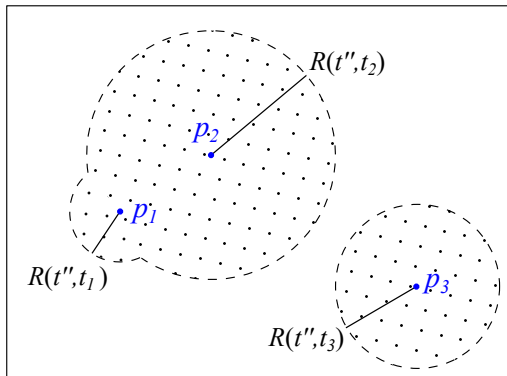


Figure 3: The region in which bubbles must nucleate at time t'' in order to reach at least one of the points p_i before time t_i .

3 Points on bubble walls

The calculations of the previous section can be adapted to points on bubble walls. Considering the bubbles as overlapping spheres, a given point of a wall has not collided if it has not been eaten by another bubble. For joint probabilities, perhaps the most direct

⁵See Ref. [31] for an alternative derivation using past light cones of the two events (t, p) , (t', p') . Although only the case of constant velocity was considered there, the derivation is valid in general.

approach is to consider, like in Sec. 2.3, the whole region of bubble nucleations at time t'' (the dotted region in Fig. 3). However, we are also interested in conditional probabilities, so we shall follow the steps of Sec. 2.2.

3.1 Probability that a point of a bubble wall remains uncollided

It is instructive to consider first the simpler case of a single point, which was first discussed in Ref. [1]. Since a single bubble has a negligible contribution to the fraction of volume occupied by bubbles, it seems, at first sight, that the probability of a given point p on its surface remaining uncollided at time t will be given by the fraction of volume $P_{fv}(t)$. However, the presence of the reference bubble to which p is attached modifies the probability that p remains in the false vacuum.

Like in Sec. 2.1, we begin by considering the probability that the point p is outside of any bubble nucleated before some time $t'' < t$. This leads to the differential equation (2) and its solution (4). Thus, we obtain the probability that p is uncollided,

$$P_u = e^{-\int_{t_c}^t dP(t'')}, \quad (20)$$

where, like before, $dP(t'')$ is the probability of p being inside a bubble nucleated between t'' and $t'' + dt''$, assuming that it is not inside any bubble nucleated before t'' . Again, for this to happen, a bubble must have nucleated at a distance smaller than $R(t'', t)$ from p (the dotted region in Fig. 1). For the present case, Fig. 4 shows the dotted region as well as the wall which contains p (represented with a solid red line). The corresponding bubble was nucleated at a certain time t_N , and we may have $t_N < t''$ or $t_N > t''$.

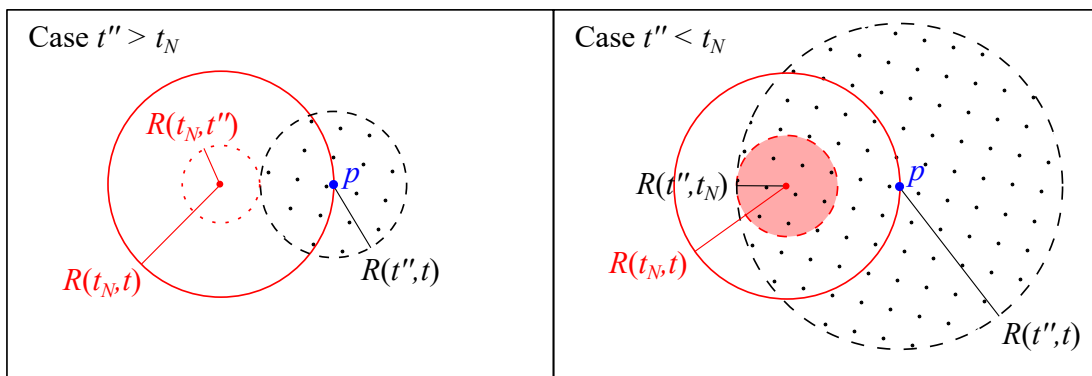


Figure 4: A bubble B nucleated at time t_N (in red) whose wall contains the point p , and the region where bubbles must nucleate at time t'' (dots) in order to reach p before time t . The shaded region corresponds to nucleations at t'' which would prevent the nucleation of the reference bubble.

We need to determine which part of the dotted region is actually available for bubble nucleation at time t'' . It is straightforward to show that, like in the previous section, the dotted region could not be invaded at time t'' by bubbles nucleated at previous times⁶ $t_{\text{prev}} < t''$. On the other hand, in the case $t'' < t_N$, a bubble nucleated at t'' may prevent

⁶In particular, in the case $t_N < t''$, the reference bubble wall containing p will be, at time t'' , just touching the limit of the dotted region, since $R(t_N, t'') + R(t'', t) = R(t_N, t)$. This is sketched with a red dotted circle in the left panel of Fig. 4.

the nucleation of the reference bubble B . This will happen if the former nucleates too close to the nucleation point of the latter; specifically, within a radius $R(t'', t_N)$ (shaded region in the the right panel of Fig. 4). Since we are assuming that bubble B exists, no bubbles can have nucleated in this region at time t'' . The probability that a bubble nucleates in the remaining part of the dotted region at a time between t'' and $t'' + dt''$ is given by⁷

$$dP(t'') = dt'' \Gamma(t'') \frac{4\pi}{3} [R(t'', t)^3 - R(t'', t_N)^3] \quad (21)$$

for $t'' < t_N$. In contrast, for $t'' > t_N$, the whole dotted region is available, and we have

$$dP(t'') = dt'' \Gamma(t'') \frac{4\pi}{3} R(t'', t)^3. \quad (22)$$

From (20-22) we obtain

$$P_u(t, t_N) = \exp[-I(t) + I(t_N)]. \quad (23)$$

The probability P_u gives also the fraction of points on the wall of the bubble nucleated at t_N which are still in the false vacuum at time t , i.e., the uncollided fraction of its surface. The result is $P_u = P_{fv}(t)/P_{fv}(t_N)$, which has a simple interpretation. Consider a large volume V . Inside this volume, a nucleation at time t_N can only occur in the available volume $VP_{fv}(t_N)$. The nucleated bubble is initially uncollided. For very large V , the probability that part of this single bubble leaves the volume $VP_{fv}(t_N)$ at later times is negligible. Nevertheless, this initial volume is invaded due to the nucleation and growth of many other bubbles, and, by time t , a smaller part of it, $VP_{fv}(t)$, remains in the false vacuum. Thus, the reference bubble is still contained in the initial volume but, in average, only a fraction $VP_{fv}(t)/VP_{fv}(t_N)$ of its points remains in the false vacuum region. This alternative derivation gives also the fraction of the bubble volume which is not covered by other bubbles.

3.2 Probability that two points of a bubble wall remain uncollided

We now consider two points p and p' on the surface of a bubble B nucleated at time t_N . We shall first find the conditional probability that p remains in the false vacuum at time t , given that p' was in the false vacuum at time t' . Following the same steps of Sec. 2.2, we obtain again

$$P_{p|p'}^S = e^{-\int_{t_c}^t dP(t'')}, \quad (24)$$

(the superscript S indicates that the two points belong to the surface of the bubble). We only need to re-calculate the probability $dP(t'')$ of p' being outside of any bubble nucleated before t'' and inside a bubble nucleated between t'' and $t'' + dt''$. Such a bubble must have nucleated within a sphere of radius $R(t'', t)$ centered at p (the dotted region in previous figures). As we have already seen, under the above conditions the dotted region is not affected by bubbles nucleated at times $t_{\text{prev}} < t''$, but we must exclude those nucleation points which would prevent the nucleation of bubble B at time t_N . Besides, since we are

⁷The forbidden (shaded) region is always completely contained inside the sphere with dots, since $R(t'', t_N) + R(t_N, t) = R(t'', t)$.

also assuming that the point p' is in the false vacuum at time t' , we must also exclude nucleation points which would affect this event.

For the sake of concreteness, let us assume that $t' \leq t$; the case $t' > t$ is similar and gives essentially the same result⁸. For $t'' > t'$, the nucleation at time t'' cannot affect events at times t_N or t' , so we have

$$dP(t'') = dt'' \Gamma(t'') \frac{4\pi}{3} R(t'', t)^3. \quad (25)$$

The case $t'' < t'$ is sketched in Fig. 5. For $t'' > t_N$ (left panel), a nucleation at time t'' cannot affect the nucleation of B at time t_N but may affect the point p' before time t' . Hence, any nucleation at time t'' must occur at a distance larger than $R(t'', t')$ from p' (i.e., outside the striped region). For $t'' < t_N$ (right panel), a nucleation at t'' may also affect the nucleation of the reference bubble. This will only happen if the nucleation at t'' occurs within a radius $R(t'', t_N)$ from the center of B (shaded region). Nevertheless, this region is fully contained in the striped region⁹. Therefore, we only have to exclude the striped region from the dotted one. Thus, for $t'' < t'$ we have

$$dP(t'') = dt'' \Gamma(t'') \left[\frac{4\pi}{3} R(t'', t)^3 - V_{\cap}(r, r', s) \right], \quad (26)$$

where V_{\cap} is the volume of the intersection of the dotted and striped regions, given by Eq. (13).

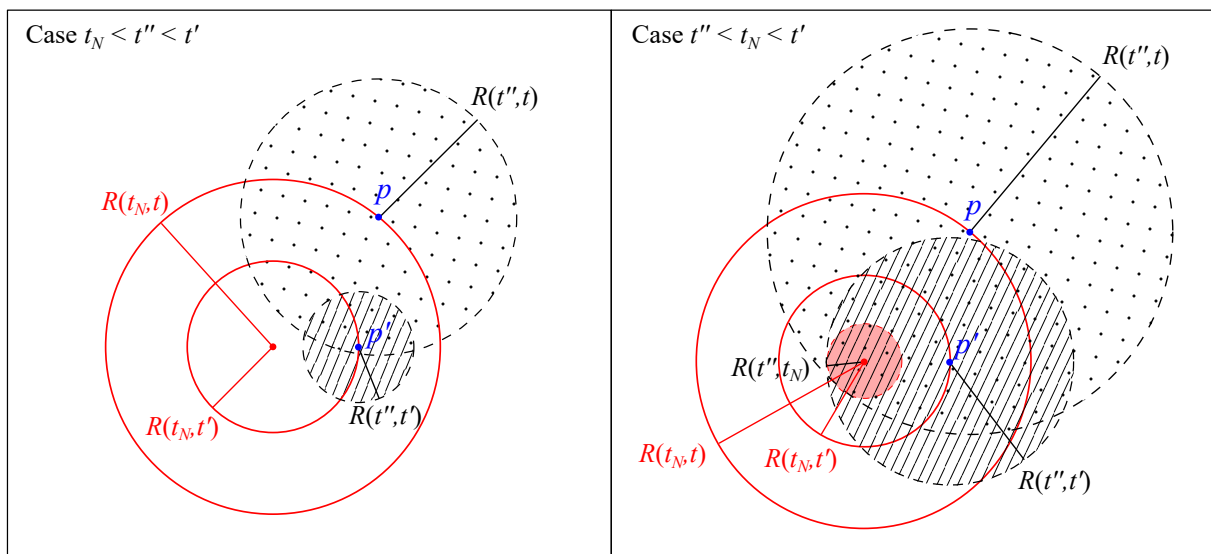


Figure 5: The reference bubble B nucleated at time t_N , at two subsequent times t' and t (in red). The dots represent the nucleations at time t'' which affect the point p before time t . Nucleations at t'' in the striped region would eat the point p' before time t' , and those in the shaded region would prevent the nucleation of B .

From Eqs. (24-26), we obtain the probability of the point p being in the false vacuum at time t under the condition that p' is in the false vacuum at time t' ,

$$P_{p|p'}^S(t, t', s) = \exp[-I(t) + I_{\cap}(t, t', s)], \quad (27)$$

⁸See footnote 3.

⁹Since $R(t'', t_N) + R(t_N, t') = R(t'', t')$. In other words, the shaded region also affects the point p' and is already taken into account.

with I_\cap given by Eq. (15). The result coincides with Eq. (14), which corresponds to the case of two arbitrary points in space. Here, the condition that p is attached to a bubble does not have more implications than the condition that p' (on the same bubble) is uncollided¹⁰. Multiplying Eq. (27) by the probability that p' was uncollided at time t' , Eq. (23), we obtain the joint probability

$$P_{p,p'}^S(t, t', t_N, s) = \exp[-I(t) - I(t') + I(t_N) + I_\cap(t, t', s)]. \quad (28)$$

As we have seen, the intersection volume V_\cap depends on the distances $r = R(t'', t)$ and $r' = R(t'', t')$, and on the separation s . The latter can be written as a function of the bubble radii

$$R \equiv R(t_N, t), \quad R' \equiv R(t_N, t'), \quad (29)$$

and the angle θ between the positions of the points p and p' relative to the bubble center (see Fig. 6),

$$s = \sqrt{R^2 + R'^2 - 2RR' \cos \theta}. \quad (30)$$

We thus have $R - R' \leq s \leq R + R'$. As we have seen in Sec. 2.2, for $s \leq r - r'$ we have $V_\cap = 4\pi r'^3/3$. In the present case, in which the two points belong to the same bubble wall, we will never actually have $s < r - r'$. Indeed, notice that

$$r - r' = R(t', t) = R - R' \leq s. \quad (31)$$

On the other hand, we may have $r + r' > s$, for which $V_\cap = 0$, so we write

$$V_\cap = \frac{\pi}{12}(r + r' - s)^2 \left[s + 2(r + r') - \frac{3(r - r')^2}{s} \right] \Theta(r + r' - s). \quad (32)$$

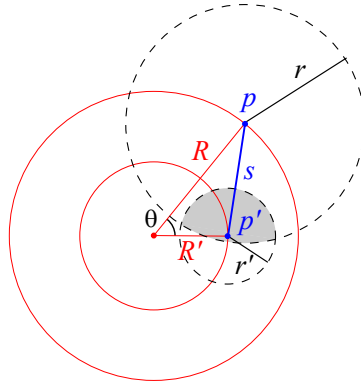


Figure 6: The intersection volume V_\cap and the separation s . The configuration corresponds to the example on the left of Fig. 5.

3.3 Points on walls of different bubbles

Now we consider the case in which the two points p and p' belong to the walls of two different bubbles B and B' , nucleated at times t_N and t'_N , respectively.

¹⁰The result would be different if p' were a random point in space. Below we consider a similar case, namely, when p' belongs to a different bubble B' .

3.3.1 General considerations

There are some conditions which will have to be taken into account eventually. In the first place, we assume that both reference bubbles exist, so neither bubble should be occupying the nucleation center of the other one. This implies that the distance l between the bubble centers must be larger than the distance travelled by a wall from one center to the other,

$$l > |R(t_N, t'_N)|. \quad (33)$$

In the second place, if the bubbles are too close, it may happen, for instance, that the point p' by time t' is already inside the bubble B . This case will be forbidden from the beginning when we consider a conditional probability which assumes that p' is uncollided at that time. On the other hand, when we consider the joint probability for both points to be uncollided at the corresponding times, the situation is not forbidden but its probability vanishes. We shall assume that we are not in this situation, which implies the condition

$$d' > R(t_N, t'), \quad (34)$$

where d' is the distance from the point p' to the center of the bubble B . Similarly, requiring that the point p is not inside the bubble B' by time t , we have the condition

$$d > R(t'_N, t), \quad (35)$$

where d is the distance from p to the center of B' . These two conditions together imply Eq. (33)¹¹. These restrictions do not affect the discussions on the nucleations at time t'' below, and the examples shown in the figures fulfill them. Nevertheless, in applying our results, it should be taken into account that the probability vanishes beyond the limits imposed by these conditions.

3.3.2 Probability that a point of a bubble wall is uncollided, given that a point of another bubble wall is uncollided

First, we assume that p' is uncollided at time t' , and we calculate the probability that p is uncollided at time t . For the sake of concreteness we shall consider only the case¹² $t \geq t'$, but we must consider the two possibilities $t'_N < t_N$ and $t_N < t'_N$. Thus, there are three possible time orderings, namely, $t'_N < t' < t_N$, $t'_N < t_N < t'$, or $t_N < t'_N < t'$ (the latter is considered in Fig. 7). The conditional probability is again given by

$$P_{pp'}^{SS'}(t, t') = e^{-\int_{t_c}^t dP(t'')} \quad (36)$$

(the superscript SS' indicates that the points belong to the surfaces S and S' of two different bubbles), and we must compute the probability $dP(t'')$ that p has not been reached by bubbles nucleated before time t'' but has been reached by a bubble nucleated in the interval $[t'', t'' + dt'']$. As before, the nucleation at t'' must occur within a sphere of radius $R(t'', t)$ centered at p (dotted region). However, some of these nucleations will also affect the point p' or the nucleations of the bubbles B or B' , and must be excluded.

¹¹Let us denote \mathbf{l} the vector going from the center of B to that of B' , \mathbf{R} the vector joining the center of B with p , and \mathbf{R}' the vector joining the center of B' with p' . We have $R = R(t_N, t)$, $R' = R(t'_N, t')$, $d = |\mathbf{l} - \mathbf{R}|$, and $d' = |\mathbf{l} + \mathbf{R}'|$ (see Fig. 8). Then, the triangular inequality gives $d \leq l + R$ and $d' \leq l + R'$. Inserting these inequalities in Eqs. (35-34) gives Eq. (33).

¹²See footnote 3.

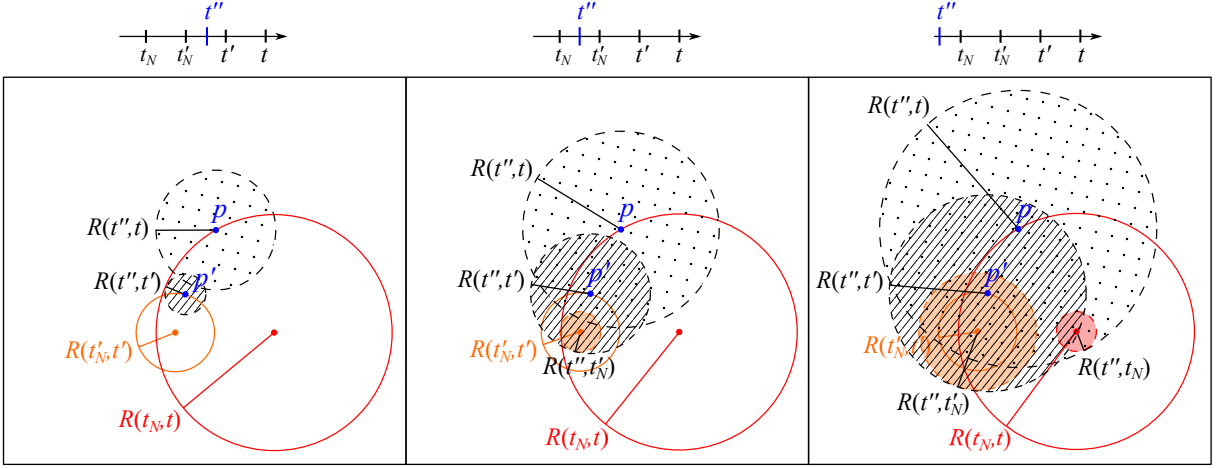


Figure 7: A bubble B nucleated at time t_N (red) and a bubble B' nucleated at time t'_N (orange). The former is drawn at time t and the latter, at time t' , with the points p and p' on each bubble surface. The black dots indicate the nucleations at time t'' which affect p at time t . Those which fall inside the striped region would also affect p' at time t' , and those in the shaded regions would affect the nucleations of B or B' .

Let us consider the time sequence $t_N < t'_N < t' < t$. The other cases are similar and lead to the same conclusion (see the appendix). Fig. 7 shows examples of the bubble configuration, corresponding to particular positions of the time t'' relative to the other times (shown in the timelines on top of each figure). The case $t'' > t'$ is the simplest one and is not shown in Fig. 7. In this case, the nucleation at t'' cannot affect the events at times t' , t'_N or t_N , and we have the whole dotted volume. Hence,

$$dP(t'') = dt'' \Gamma(t'') \frac{4\pi}{3} R(t'', t)^3 \quad (t'' > t'). \quad (37)$$

In the case $t'_N < t'' < t'$ (left panel of Fig. 7), a bubble nucleated at time t'' may have eaten the point p' by time t' , so we must exclude the sphere of radius $R(t'', t')$ centered at p' (striped region). We thus have

$$dP(t'') = dt'' \Gamma(t'') \left[\frac{4\pi}{3} R(t'', t)^3 - V_\cap \right] \quad (t'_N < t'' < t'), \quad (38)$$

where V_\cap is the volume of the intersection of the striped and dotted spheres, which is given by Eq. 13.

For $t_N < t'' < t'_N$ (shown in the central panel of Fig. 7), the nucleation at t'' may also prevent the nucleation of bubble B' . Nevertheless, like in the previous section, the region which can affect this event (light orange shade in Fig. 7) is completely contained within the striped region, which is already excluded in Eq. (38). Therefore, nothing changes when t'' becomes smaller than t'_N ,

$$dP(t'') = dt'' \Gamma(t'') \left[\frac{4\pi}{3} R(t'', t)^3 - V_\cap \right] \quad (t_N < t'' < t'_N). \quad (39)$$

Finally, for $t'' < t_N$ (right panel), the nucleation at t'' may also prevent the nucleation of bubble B . Therefore, we must exclude the sphere of radius $R(t'', t_N)$ around the center

of B (pink shade), as well as the striped region. We thus have

$$dP(t'') = dt''\Gamma(t'') \left[\frac{4\pi}{3}R(t'', t)^3 - \frac{4\pi}{3}R(t'', t_N)^3 - V_\cap + V'_\cap \right] \quad (t'' < t_N). \quad (40)$$

Here, we have first subtracted the volume of the pink region, which is completely contained inside the dotted region, then we have subtracted the intersection volume V_\cap of the striped and dotted regions. The volume V'_\cap is a correction for the case in which the striped region overlaps with the pink region, like in the example of Fig. 7. This volume must be added in order to avoid subtracting twice their intersection. This happens when the distance d' between p' and the center of B is short enough. Thus, V'_\cap depends on d' and on the radii of the two spheres, $r' = R(t'', t')$ and $r_N \equiv R(t'', t_N)$ (see Fig. 8), and we have¹³

$$V'_\cap = \frac{\pi}{12}(r' + r_N - d')^2 \left[d' + 2(r' + r_N) - \frac{3(r' - r_N)^2}{d'} \right] \Theta(r' + r_N - d'). \quad (41)$$

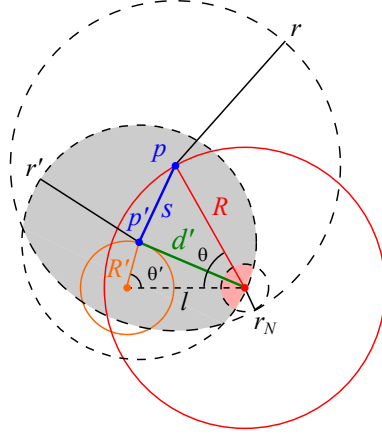


Figure 8: The intersection volumes V_\cap (gray) and V'_\cap (pink), and the distances s and d' . This specific configuration corresponds to the case on the right panel of Fig. 7.

Inserting these results in Eq. (36), we obtain

$$P_{p|p'}^{SS'}(t, t', s, d', t_N) = \exp[-I(t) + I(t_N) + I_\cap(t, t', s) - I'_\cap(t', t_N, d')], \quad (42)$$

where I_\cap is the integral given by Eq. (15), and I'_\cap is a similar integral involving V'_\cap . According to Eq. (40), the upper limit of this integral is t_N . However, if we take into account the possibility $t' < t_N$ (not considered in the example used for this derivation), we must write (see the appendix for details)

$$I'_\cap(t', t_N, d') = \int_{t_c}^{\min\{t_N, t'\}} dt''\Gamma(t'')V'_\cap(r', r_N, d'). \quad (43)$$

¹³The Heaviside function takes into account the fact that for large enough separation the intersection is empty. On the other hand, the condition (34), $d' > R(t_N, t') = R(t'', t') - R(t'', t_N) = r' - r_N$, implies that the sphere of radius r_N will never be contained completely inside that of radius r' , except as a limit.

The distance s between p and p' is no longer given by Eq. (30). We may relate the relevant distances with the orientations of the points on each bubble surface,

$$s^2 = l^2 + R^2 + R'^2 - 2lR' \cos \theta' - 2lR \cos \theta + 2RR'(\sin \theta \sin \theta' \cos \phi - \cos \theta \cos \theta'), \quad (44)$$

$$d' = \sqrt{R'^2 + l^2 - 2R'l \cos \theta'}, \quad d = \sqrt{R^2 + l^2 - 2Rl \cos \theta}, \quad (45)$$

where $R \equiv R(t_N, t)$, $R' \equiv R(t'_N, t')$, l is the separation between the bubble centers, the angles θ and θ' (which are in the interval $[0, \pi]$) correspond to the orientations of the points p and p' on each bubble with respect to the axis joining the two centers (see Fig. 8), and ϕ (in the interval $[0, 2\pi]$) is the angle between the projections of these directions on the plane perpendicular to the axis. Although Eq. (42) does not depend on d , this distance appears in the condition (35). Indeed, in the derivation of $P_{p|p'}^{SS'}$ we have assumed that the conditions (34-35) are fulfilled. The assumption $d' > R(t'_N, t')$ is correct, since the conditional probability assumes that the point p' is uncollided. On the other hand, the condition $d > R(t'_N, t)$ is not necessarily valid. If it is not fulfilled, the point p at time t is inside bubble B' , and the probability just vanishes, so we must multiply Eq. (42) by the Heaviside function

$$\Theta(d - R(t'_N, t)). \quad (46)$$

It is interesting to consider the the limit in which B and B' nucleate at the same time and very close to each other. For $l = 0$, Eq. (45) gives $d' = R'$ and s becomes the same as for the single-bubble case, i.e., Eq. (44) becomes Eq. (30). Besides, for $t_N = t'_N$ we have $r' - d' = R(t'', t') - R(t'_N, t') = R(t'', t'_N) = r'_N = r_N$. Using this result, the volume V'_\cap becomes $V'_\cap = \frac{4\pi}{3} r_N^3$. Hence, I'_\cap cancels with $I(t_N)$ in Eq. (42), and we obtain $P_{p|p'}^{SS'}(t, t', s) = \exp[-I(t) + I_\cap(t, t', s)]$, which coincides with Eq. (28), i.e., the probability $P_{p|p'}^S(t, t', s)$ for two points on the same bubble wall. This was to be expected, since in this limit the two bubbles are almost coincident. However, we must also take into account Eq. (46). In particular, in this limit many points on each surface must be eaten by the other bubble (here, we are assuming that p' is not). In the case $t'_N = t_N$ Eq. (46) becomes $\Theta(d - R)$. For $l \rightarrow 0$ we have $d \rightarrow R$, so we must be careful with the limit. For $l \ll R$ Eqs. (45) can be written

$$d - R = -l \cos \theta, \quad d' - R' = -l \cos \theta'. \quad (47)$$

Hence, the Heaviside function *vanishes* for $\cos \theta > 0$, i.e., for $\theta < \pi/2$. This is because, in this limit, a half of bubble B is inside B' .

3.3.3 Probability that a point on a bubble wall is uncollided, in the presence of another bubble

To obtain the joint probability that a point p on the surface of B and a point p' on the surface of B' remain uncollided at times t and t' , respectively, we only have to multiply $P_{p|p'}^{SS'}$ by the probability that the point p' on the wall of B' is uncollided at time t' (without any condition on the point p). This probability was obtained in Sec. 3.1 and is given by Eq. (23). However, the conditions are different in the present case, since we assume the existence of another bubble, B , at a certain distance from B' (otherwise, we cannot ask whether the point p on B is uncollided). Therefore, we must consider the probability that p' on B' is uncollided at time t' , in the presence of the bubble B . This probability may be also of interest on its own.

Following the derivation of Sec. 3.1, we consider the region of nucleations at time t'' which affect p' at time t' (in Fig. 4 this was the dotted region but in Fig. 7 it is represented by a striped region). Like before, we need to exclude nucleations at t'' which affect the nucleation of the reference bubble B' at t'_N (the orange region in Fig. 7), but also those which prevent the nucleation of B at t_N (the pink region). We thus obtain

$$P_{p'|B}^u(t', t'_N, t_N, d') = \exp[-I(t') + I(t'_N) + I'_\cap(t', t_N, d')]. \quad (48)$$

The first two terms in the exponent are like in Eq. (23). However, the probability that p' (on the surface of B') is uncollided depends also on its distance to the center of B and the nucleation time of the latter. In this derivation we have assumed that Eq. (34) is fulfilled. Therefore, Eq. (48) does not take into account the possibility that bubble B has eaten the point p' , and we must add the factor

$$\Theta(d' - R(t_N, t')). \quad (49)$$

3.3.4 Probability that two points on the walls of different bubbles are uncollided

The joint probability that both points are uncollided is given by the product of Eqs. (48) and (42),

$$P_{p,p'}^{SS'}(t, t', t_N, t'_N, s) = \exp[-I(t) - I(t') + I(t_N) + I(t'_N) + I_\cap(t, t', s)]. \quad (50)$$

The integral $I'_\cap(t', t_N, d')$ has canceled out, so this expression depends only on the point separation and not on the bubble separation l . The result is very similar to the single-bubble probability, Eq. (28), except for the extra term $I(t'_N)$ in the exponent. However, we remark that if any of the conditions (34-35) is not fulfilled, one of the points has been eaten by the other bubble, and the probability actually vanishes. Therefore, Eq. (50) must be multiplied by the Heaviside functions

$$\Theta(d - R(t'_N, t))\Theta(d' - R(t_N, t')). \quad (51)$$

To see the dependence with l , let us consider, for simplicity, the case $t'_N = t_N$ and $t' = t$, so that we have two bubbles of the same size. In this case, Eq. (51) becomes $\Theta(d - R)\Theta(d' - R)$. For $l > R$, Eqs. (45) give $l - R < d < l + R$, and the same for d' . For $l > 2R$, both d and d' are larger than R , so the Heaviside functions give a factor 1. Thus, for large l , the probability is given by Eq. (50), which depends only on the point separation s . On the other hand, for $l < 2R$ the two bubbles overlap, and some points will have zero probability of being uncollided (depending on d and d'). For $l < R$, Eqs. (45) give $R - l < d < R + l$, and for $l \ll R$ we have Eqs. (47) which, inserted in (51) imply $\theta > \pi/2, \theta' > \pi/2$. This is because, as already discussed, when the two bubbles almost coincide, a half of each bubble is inside the other bubble.

4 Some particular cases and applications

We shall now consider some basic quantities which are related to the physical consequences of the phase transition and are obtained from the probabilities derived above. For concrete computations, we shall use a simple model for the phase transition, namely, a simultaneous nucleation and a constant wall velocity,

$$\Gamma(t) = n_b \delta(t - t_*), \quad R(t', t) = v(t' - t). \quad (52)$$

4.1 The envelope of uncollided walls

We shall begin by considering the (uncollided) wall area. For a given bubble of radius R , the locus of its uncollided wall is a subset of the sphere of radius R . A given point on the sphere is characterized by two angles θ, ϕ by means of the parametrization $\mathbf{r} = R\hat{r}$, where $\hat{r} = (\sin\theta \cos\phi, \sin\theta \sin\phi, \cos\theta)$. The uncollided wall can be characterized by the indicator or characteristic function

$$1_S(\theta, \phi) = \begin{cases} 1 & \text{if } \mathbf{r} \in S, \\ 0 & \text{if } \mathbf{r} \notin S. \end{cases} \quad (53)$$

Thus, the area of this bubble wall can be written in the form¹⁴

$$S = R^2 \int_0^{2\pi} d\phi \int_0^\pi d\theta \sin\theta 1_S(\theta, \phi). \quad (54)$$

If we regard the characteristic function as a stochastic variable and average over bubbles of the same radius R , we have

$$\langle S \rangle = R^2 \int_0^{2\pi} d\phi \int_0^\pi \sin\theta d\theta \langle 1_S(\theta, \phi) \rangle. \quad (55)$$

For each direction \hat{r} , we have two possible values of $1_S(\theta, \phi)$, with probabilities $P_{\hat{r}}(1)$ and $P_{\hat{r}}(0) = 1 - P_{\hat{r}}(1)$, and we have $\langle 1_S(\theta, \phi) \rangle = P_{\hat{r}}(1)$. This is the probability that the point represented by \hat{r} is uncollided, which is given by Eq. (23) and is independent of the direction, $P_{\hat{r}}(1) = P_u(t, t_N) = e^{-I(t)+I(t_N)}$. Thus, the average uncollided area of a bubble of radius R is given by

$$\langle S \rangle = 4\pi R^2 e^{-I(t)+I(t_N)}. \quad (56)$$

To obtain the total surface in a given volume V , we must multiply Eq. (56) by the number of bubbles of radius R in this volume, and then integrate over R . According to Eq. (1), the bubbles of radius R are those which were nucleated at the time $t_N(R, t)$ such that $R = \int_{t_N}^t v(t'') dt''$. Thus, at time t , the bubbles which have radii between R and $R + dR$ are those nucleated between $t_N - dt_N$ and t_N . The number of these bubbles is¹⁵

$$dN = \Gamma(t_N) V P_{fv}(t_N) dt_N. \quad (57)$$

Since $P_{fv}(t_N) = e^{-I(t_N)}$, we have

$$\langle S_{\text{tot}} \rangle = \int dN \langle S \rangle = V e^{-I(t)} \int_{t_c}^t dt_N \Gamma(t_N) 4\pi R(t_N, t)^2. \quad (58)$$

¹⁴We use the same notation S for the locus of the uncollided wall and its area.

¹⁵Using also $dR = -v(t_N) dt_N$, we may obtain the distribution of bubble sizes $dn/dR = V^{-1} dN/dR$. Another quantity of interest is the volume-weighted distribution of bubble sizes, $(4\pi/3)R^3 dn/dR$, which is associated to the energy that has been released in bubbles of a given size. The surface-weighted size distribution $4\pi R^2 dn/dR$ may also be of interest, depending on the application. In this case, it would be perhaps more appropriate to use the *uncollided* surface as weight, $\langle S \rangle dn/dR$. We shall not discuss size distributions here, since we shall use the model (52), for which all the bubbles have the same radius.

As discussed in Sec. 1, for phenomena which depend on the bubble walls, the important measure of progress (rather than the volume fraction f_b) will be the fraction of uncollided wall area, $f_S(t)$, which is obtained by dividing Eq. (58) by $V \int dN 4\pi R^2$,

$$f_S(t) = \frac{e^{-I(t)} \int_{t_c}^t dt_N \Gamma(t_N) R(t_N, t)^2}{\int_{t_c}^t dt_N e^{-I(t_N)} \Gamma(t_N) R(t_N, t)^2}. \quad (59)$$

In Ref. [1], the energy-weighted fraction $f_E(t)$ is also defined, by replacing $R(t_N, t)^2$ with $R(t_N, t)^3$ in the numerator and denominator of Eq. (59). It is to be expected that different measures of progress such as f_S , f_E , or $P_{fv} = 1 - f_b$ (all of which vary from 1 to 0 throughout the phase transition) are qualitatively similar. In Ref. [1] it was found that, for the case of an exponentially growing nucleation rate, $P_{fv}(t)$ and $f_E(t)$ are very similar even quantitatively. For the delta-function rate (52) we have

$$\langle S_{\text{tot}} \rangle = V n_b 4\pi R(t_*, t)^2 e^{-I(t)}, \quad (60)$$

with

$$I(t) = n_b \frac{4\pi}{3} R(t_*, t)^3, \quad (61)$$

while the denominator in Eq. (59) is given by $V n_b 4\pi R(t_*, t)^2$. Therefore, we have $f_S(t) = e^{-I(t)} = P_{fv}(t)$. The same happens with $f_E(t)$; i.e., for simultaneous nucleation all these measures of progress coincide. For this model, a convenient unit of length is the characteristic distance $d_b \equiv n_b^{-1/3}$ (the ‘‘average’’ bubble separation), and, for constant velocity, a convenient unit of time is the associated value $\Delta t_b = d_b/v$ (which gives an estimate for the duration of the phase transition). Thus, we may write

$$f_S(t) = \exp \left[-\frac{4\pi}{3} \left(\frac{t - t_*}{\Delta t_b} \right)^3 \right]. \quad (62)$$

Hence, in units of the time scale Δt_b , this function does not depend explicitly on the wall velocity. In a volume $V = d_b^3$, the average wall area is given by

$$\frac{\langle S_{\text{tot}} \rangle}{d_b^2} = 4\pi \left(\frac{t - t_*}{\Delta t_b} \right)^2 \exp \left[-\frac{4\pi}{3} \left(\frac{t - t_*}{\Delta t_b} \right)^3 \right]. \quad (63)$$

In Fig. 9 we plot f_S and $\langle S_{\text{tot}} \rangle$ as functions of time. The vertical lines indicate some representative times near the beginning, the middle, and the end of the transition. We see that, when bubbles occupy a 1% of space, the area in their walls is already $0.22d_b^2$, which is more than a 10% of its maximum value. This is because of the high surface/volume ratio for small bubbles, which, moreover, are uncollided. The maximum presence of walls occurs approximately in the middle of the phase transition, when the fraction of volume is $f_b \simeq 0.49$. Finally, when only a 1% of space remains in the false vacuum, the uncollided area is approximately $0.13d_b^2$, which is still a 7% of its maximum. This relatively high value (compared to f_S) occurs because f_S is a fraction of an ever-increasing surface.

4.2 Time correlations in the envelope

The function $\langle S_{\text{tot}}(t) \rangle$ describes the turning on and off of the system of walls which sources several of the consequences of the phase transition. However, as already mentioned, in

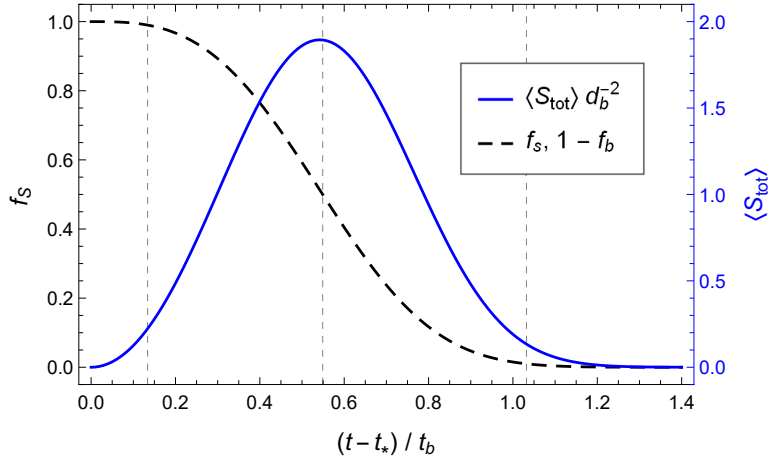


Figure 9: The fraction of volume and of surface, $f_s = 1 - f_b$, and the remaining wall area $\langle S_{\text{tot}} \rangle$ at time t . The vertical lines correspond to the values $f_b = 0.01, 0.5$ and 0.99 .

some cases the relevant quantity will be the time correlation $\langle S_{\text{tot}}(t)S_{\text{tot}}(t') \rangle$, or even correlations between individual bubbles or between parts of bubbles. As we have seen, in the case of simultaneous nucleation, the total uncollided area is proportional to that of a single bubble, and we may also expect a similar relation for the surface correlations. The total surface involves a sum over individual bubbles, $S_{\text{tot}} = \sum_i S_i$, and we may write

$$S_{\text{tot}}(t)S_{\text{tot}}(t') = \sum_i S_i(t)S_i(t') + \sum_i \sum_{j \neq i} S_i(t)S_j(t'). \quad (64)$$

Taking the ensemble average, the terms in the first sum involve time correlations of a single bubble. These terms will depend only on t, t' and the nucleation time t_N , but not on the bubble position. Therefore, in a volume V , we may evaluate the sum by replacing $\sum_i \rightarrow V \int \Gamma(t_N) P_{fv}(t_N) dt_N$, like we did in Sec. 4.1. In the case of simultaneous nucleation, this gives a factor Vn_b . On the other hand, the terms in the double sum in Eq. (64) will depend on the bubble separation l . Therefore, the sum over j can be replaced by the integral $4\pi \int dl l^2$. The result does not depend on the bubble positions, and then the sum over i gives again a factor Vn_b . Below we consider these two contributions separately.

Let us first consider a bubble at different times t, t' . The uncollided area at each time is given by Eq. (54), and we have

$$\langle S(t)S(t') \rangle = R^2 R'^2 \int_0^{2\pi} d\phi' \int_0^\pi \sin \theta' d\theta' \int_0^{2\pi} d\phi \int_0^\pi \sin \theta d\theta \langle 1_{S(t)}(\theta, \phi) 1_{S(t')}(\theta', \phi') \rangle. \quad (65)$$

The angles correspond to directions \hat{r}, \hat{r}' indicating points p, p' on the surfaces $S(t)$ and $S(t')$, respectively. For each pair \hat{r}, \hat{r}' , the product $1_{S(t)} 1_{S(t')}$ takes the value 0 or 1, the latter with probability $P_{\hat{r}, \hat{r}'}(1) = P_{p, p'}^S(t, t', t_N, s)$ given by Eq. (28). This probability depends on a single angle, namely, that between \hat{r} and \hat{r}' . Using the relation (30) for the point separation s , we obtain¹⁶

$$\langle S(t)S(t') \rangle = 8\pi^2 R R' e^{-I(t) - I(t') + I(t_N)} \int_{R'-R}^{R'+R} ds s e^{I \cap (t, t', s)}, \quad (66)$$

¹⁶In Eq. (65) we measure the angle θ from \hat{r}' , and we have $s ds = R R' \sin \theta d\theta$.

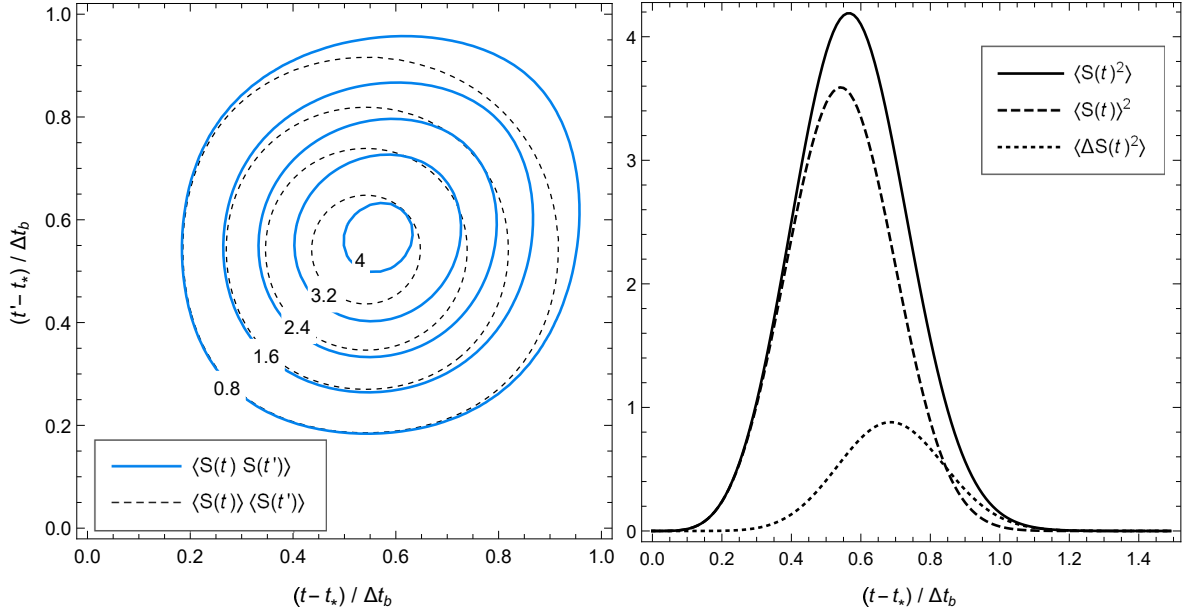


Figure 10: Surface correlation of a bubble wall at two times, in units of d_b^4 . Left panel: contours of $\langle S(t)S(t') \rangle$ and $\langle S(t) \rangle \langle S(t') \rangle$ Right panel: the equal-time values and their difference.

where I_\cap is given by Eq. (15). For our model with a delta-function rate we have $t_N = t_*$, $I(t_*) = 0$, and $I_\cap = n_b V_\cap$, with

$$V_\cap = \frac{\pi}{12} (R + R' - s)^2 \left[s + 2(R + R') - \frac{3(R' - R)^2}{s} \right], \quad (67)$$

while $I(t)$ is given by Eq. (61). At equal times we have $R' = R$, and the expression for V_\cap is simpler,

$$V_\cap = \frac{\pi}{12} (2R - s)^2 (s + 4R). \quad (68)$$

In any case, the integral (66) must be computed numerically, even for constant wall velocity, in which case we have $R = v(t - t_*)$.

In Fig. 10 we compare the functions $\langle S(t)S(t') \rangle$ and $\langle S(t) \rangle \langle S(t') \rangle$. The latter has a simpler expression¹⁷ and could be used as an approximation for the former. Such an approximation corresponds to assuming that the two surfaces are uncorrelated. We see that these quantities are quite similar. In particular, the approximation is very good initially (i.e., for small values of $t - t_*$ and $t' - t_*$). However, they depart at later times, where the uncorrelated function tends to zero more rapidly. In the right panel, the variance $\langle \Delta S^2 \rangle$, where $\Delta S = S - \langle S \rangle$, is also shown. The left panel of Fig. 11 shows the covariance $\langle \Delta S(t) \Delta S(t') \rangle$. In the right panel we compare the function $\langle S(t)S(t') \rangle$ with $\sqrt{\langle S(t)^2 \rangle \langle S(t')^2 \rangle}$. The latter is the result we would obtain if $S(t)$ and $S(t')$ were maximally correlated. Since Eqs. (66-67) are simpler for equal times, this function can also be used as an approximation for the former. By definition, both coincide at $t = t'$, so this approximation is better than the uncorrelated one at later times. On the other hand, it deviates for large $|t - t'|$.

¹⁷In particular, it can be obtained analytically from Eq. (56), which in this model gives $\langle S \rangle = 4\pi R^2 e^{-I}$.

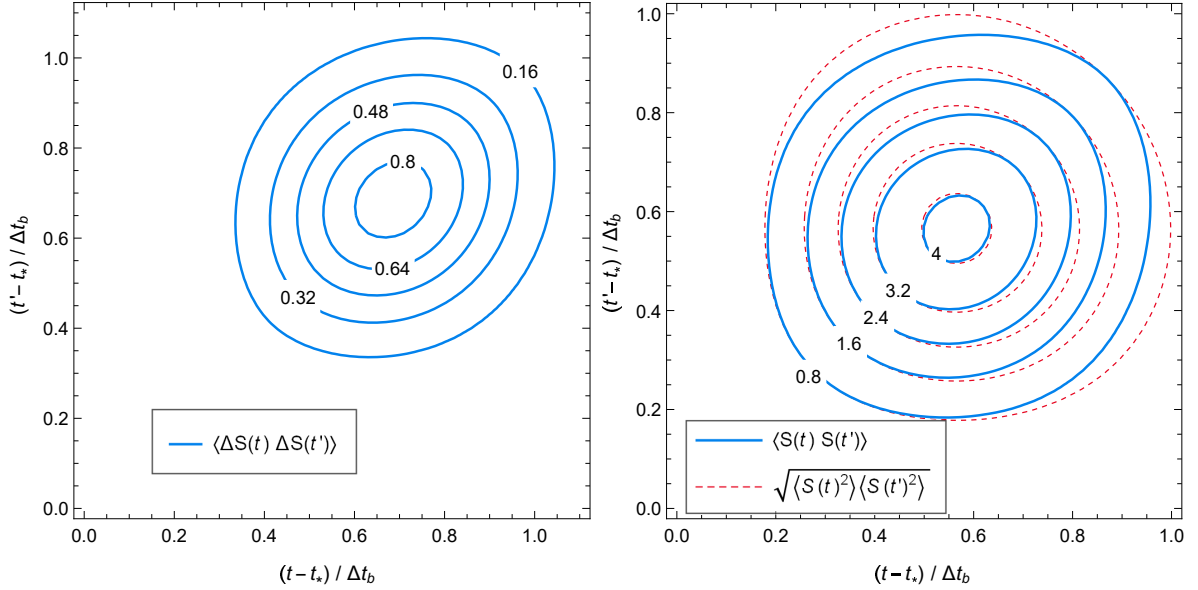


Figure 11: Left panel: contours of $\langle \Delta S(t) \Delta S(t') \rangle$ for a bubble wall at different times. Right panel: contours of $\langle S(t) S(t') \rangle$ and $\sqrt{\langle S(t)^2 \rangle \langle S(t')^2 \rangle}$. The areas are in units of d_b^2 .

If we consider two different bubbles, whose centers are a distance l apart, we may repeat the same steps which lead to Eq. (66). The only difference is that now we have two surfaces belonging to different bubbles, so we replace $S(t')$ with $S'(t')$ in Eq. (65), and the probability $P_{\hat{r}, \hat{r}'}(1)$ is given by Eqs. (50-51). We thus have

$$\langle 1_{S(t)}(\theta, \phi) 1_{S'(t')}(\theta', \phi') \rangle = P_{p, p'}^{SS'}(t, t', t_N, t'_N, s) \Theta(d - R(t'_N, t)) \Theta(d' - R(t_N, t')). \quad (69)$$

We shall continue using the model in which all bubbles nucleate simultaneously, so we have $t_N = t'_N = t_*$ and $I(t_*) = 0$. We obtain

$$\begin{aligned} \langle S(t) S'(t') \rangle &= 2\pi R^2 R'^2 e^{-n_b \frac{4\pi}{3} (R^3 + R'^3)} \int_0^{2\pi} d\phi \int_0^\pi d\theta \sin \theta \int_0^\pi d\theta' \sin \theta' \\ &\times \exp[n_b V_\cap(R, R', s)] \Theta(d - R) \Theta(d' - R'). \end{aligned} \quad (70)$$

We could also change the variables of integration from the angles to the distances s, d, d' through Eqs. (44-45). The result depends on the bubble separation l .

We show the result in Fig. 12. We consider the deviations $\Delta S, \Delta S'$, and we plot only the equal-time case. In the left panel, the covariance¹⁸ $\langle \Delta S(t) \Delta S'(t) \rangle$ is plotted as a function of the bubble radius R , or, equivalently, as a function of time, since we have $R/d_b = (t - t_*)/\Delta t_b$. The curves of different colors correspond to various values of the bubble separation l . We see that the correlation vanishes for large l , i.e., we have $\langle S(t) S'(t) \rangle \rightarrow \langle S(t) \rangle \langle S'(t) \rangle$ for $l \rightarrow \infty$. On the other hand, the maximal correlation is attained for $l \rightarrow 0$. This is also appreciated in the right panel, which shows the covariance as a function of l for a few values of R . In all these curves, there is a sudden change in the behavior at the point $l = 2R$, i.e., when the two bubbles come into contact. For $l < 2R$, the two bubbles overlap, so a part of their surface is surely collided. One could expect

¹⁸In the general case we have $\langle \Delta S(t) \Delta S'(t') \rangle = \langle S(t) S'(t') \rangle - \langle S(t) \rangle \langle S'(t') \rangle$. Notice that $\langle S'(t') \rangle = \langle S(t') \rangle$. Thus, for equal times we have $\langle \Delta S(t) \Delta S'(t) \rangle = \langle S(t) S'(t) \rangle - \langle S(t) \rangle^2$.

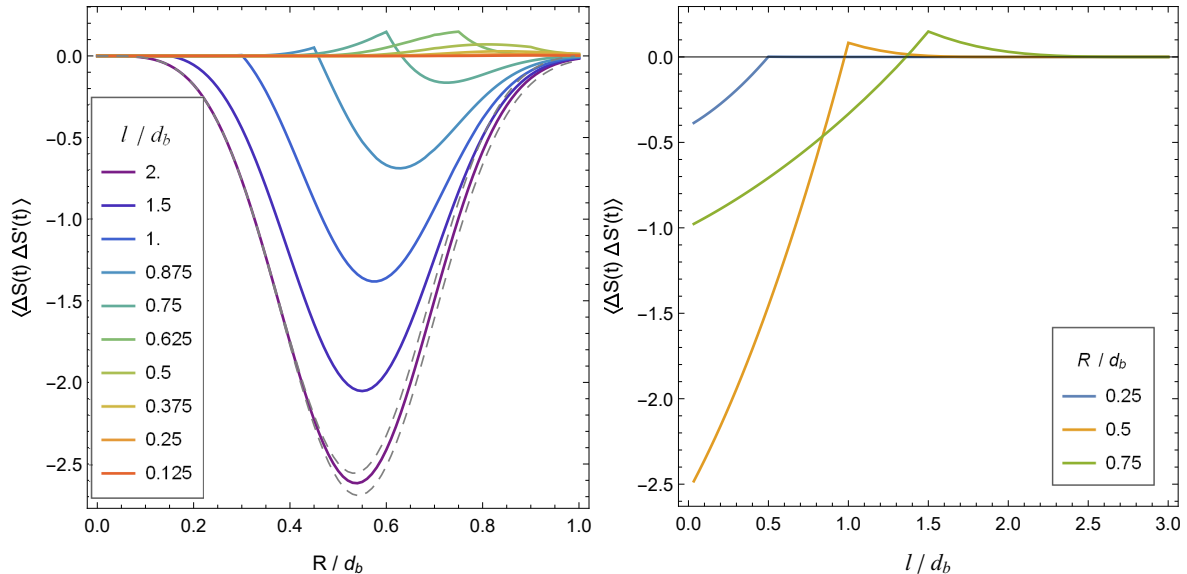


Figure 12: The equal-time function $\langle \Delta S(t) \Delta S'(t) \rangle$ (in units of d_b^4) for two bubbles separated a distance l , as a function of the bubble radius (left panel) and as a function of the bubble separation (right panel). The dashed curves in the left panel correspond to the functions $\langle S(t)^2 \rangle / 4 - \langle S(t) \rangle^2$ (upper curve) and $-3\langle S(t) \rangle^2 / 4$ (lower curve).

that for $l \rightarrow 0$ the quantity $\langle S(t) S'(t) \rangle$ would match the value $\langle S(t) S(t) \rangle$. However, in this limit, half of each bubble is surely collided, so a better guess would be $\langle S(t)^2 \rangle / 4$. This value is indicated by the upper dashed line in the left panel of Fig. 12. We see that this curve does not coincide with the limit $l = 0$ for different bubbles. The lower dashed line corresponds to the approximation $\langle S(t) \rangle^2 / 4$.

4.3 Correlation between different parts of a bubble wall

Conditional and joint probabilities for different points on a bubble wall to be or not collided are basic ingredients in the calculation of the dynamics of bubble intersections which enter the mechanism of defect trapping. As a simple application of our results, we shall consider these probabilities for two points at a given time.

In the first place, Eq. (23) gives the probability that a single point on the wall remains uncollided, $P_u(t, t_N) = \exp[-I(t) + I(t_N)]$. This probability depends on the nucleation time and, hence, on the bubble radius. For the delta-function nucleation rate, though, we have $t_N = t_*$ for all bubbles, so we have $P_u(t, t_N) = e^{-I(t)} = f_S(t)$.

Let us now consider, on the wall of a bubble at a given time t , the probability that a point p is uncollided, assuming that another point p' is uncollided, which is given by Eq. (27). We must use Eqs. (29-32) for the case $t' = t$. For simultaneous nucleation, I is given by Eq. (61), $I_\cap = n_b V_\cap$, with V_\cap given by Eq. (68), and $s = R\sqrt{2}(1 - \cos \theta) = 2R \sin(\theta/2)$. Thus, we obtain

$$P_{p|p'}^S(t, \theta) = \exp \left[-\frac{4\pi}{3} \left(\frac{t - t_*}{\Delta t_b} \right)^3 \left(\frac{3}{2} \sin(\theta/2) - \frac{1}{2} \sin^3(\theta/2) \right) \right]. \quad (71)$$

The joint probability that both p and p' are in the false vacuum is given by $P_{p,p'}^S(t, \theta) = e^{-I(t)} P_{p|p'}(t, \theta)$. We show this result in Fig. 13. At the beginning of the phase transition

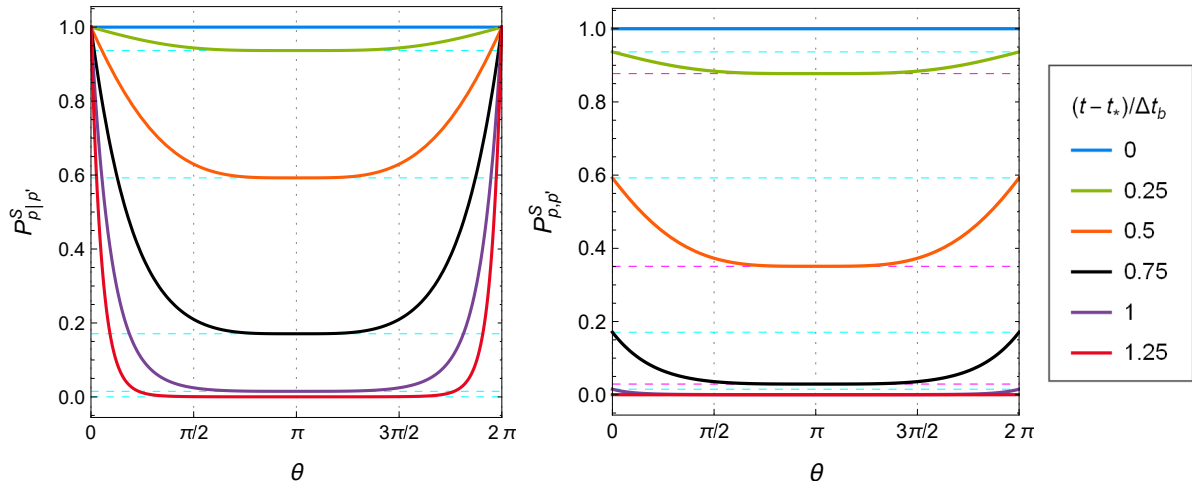


Figure 13: Conditional probability (left) and joint probability (right) for two points on a bubble wall to be uncollided, as a function of the angle of separation. The horizontal dashed cyan lines indicate the value of $P_u(t) = f_S(t)$. The horizontal dashed magenta lines indicate the value $P_u(t)^2$.

we have $P_{p,p'}^S = P_{p|p'}^S = 1$, since the two points are uncollided because the whole bubble is isolated. By the end of the phase transition, the probability that both points are uncollided vanishes unless we assume that one of them is uncollided. In this case (left panel), the probability will not vanish for $\theta \simeq 0$. At intermediate times, assuming that p' is uncollided, the probability that p is also uncollided falls with the distance from p' (the maximum distance corresponds to $\theta = \pi$). As p departs from p' , the probability approaches the value $P_u(t)$ (the probability for an arbitrary point), indicating that the correlation is lost. In contrast, the joint probability for both points to be uncollided takes the value $P_u(t)$ when the points are very close, while for large separations it approaches the uncorrelated value $P_u(t)P_u(t)$.

5 Discussion

We have studied bubble wall correlations in a cosmological phase transition using a statistical treatment of the bubble kinematics. This kinematics is based on the assumptions of a homogeneous nucleation rate $\Gamma(t)$ and a homogeneous wall velocity $v(t)$ (the latter implies that bubbles are spherical and that all expand with the same velocity). Although these assumptions are very common, they are not always valid. The nucleation rate is certainly homogeneous in the case of a vacuum transition, where Γ is of the form $\Gamma = Ae^{-S}$, with A and S constant [3, 4]. Furthermore, the wall quickly approaches the asymptotic value $v = 1$. In the case of a thermal transition, Γ has a similar form, but A and S depend on the temperature [7, 8]. In general, the bubble walls reach a terminal velocity in a time which is much shorter than the total duration of the phase transition, but this velocity also depends on the temperature. In a phase transition mediated by detonations [33], the latent heat that is released at the bubble walls only reheats the plasma behind the walls (inside the bubbles), so Γ and v are not affected by temperature inhomogeneities.

In contrast, for deflagrations [34, 35, 36], the fluid is perturbed in front of the bubble walls, and perturbations coming from different bubbles cause inhomogeneous reheating.

Nevertheless, in the case of very slow deflagrations, the released latent heat is distributed with a relatively high speed, so a homogeneous reheating can be assumed [37]. In the intermediate case of deflagrations which are not very slow ($0.1 \lesssim v \lesssim 0.6$), a shock wave moving at approximately the speed of sound reheats the plasma in front of the wall. In this case, the kinematic treatment can still be simplified by taking into account that in a region of radius $R_{\text{sh}} \approx (c_s/v)R$ around each bubble the nucleation rate vanishes [38]. This approximation assumes that the reheating caused by a single bubble is enough to turn off the nucleation rate, so the inhomogeneous temperature resulting from several shock waves is irrelevant. However, some approximation is still required for the velocity, which is not as sensitive to temperature. Our results can in principle be adapted to such a treatment. On the other hand, a deflagration wall may corrugate due to hydrodynamic instabilities [39, 40, 41]. These instabilities will grow from random fluctuations, and a different statistical treatment of the walls will be necessary in this case.

Assuming a homogeneous temperature, the time dependence of Γ and of v will depend on the function $T(t)$. For detonations, the reheating can be ignored until the end of the phase transition, so $T(t)$ is determined by the adiabatic expansion. In this case, an exponentially growing nucleation rate is generally a good approximation, and the wall velocity can be assumed to be constant during the short time of bubble growth. For deflagrations, the evolution of T is more involved (even assuming a homogeneous reheating). In general, there is a supercooling stage followed by a sudden reheating. Due to the high sensitivity of the nucleation rate, Γ turns off as soon as the reheating begins. In this case, a reasonable approximation is to assume that all bubbles nucleate when Γ reaches its maximum value [42]. The wall velocity also decreases due to reheating, but its evolution is less simple. Nevertheless, analytic approximations for $v(t)$ exist [43]. In our explicit examples, we have considered a toy model in which all bubbles nucleate simultaneously but the wall velocity is constant. We expect that this simple model reflects all the qualitative features of the quantities we have discussed. For instance, we have mentioned that different measures of progress of the phase transition are, in general, similar, and in this model we have, indeed, $f_S(t) = 1 - f_b(t)$. Similarly, we expect that in general the maximum surface of uncollided walls will occur about the middle of the phase transition, since in this model it happens when the fraction of volume is $f_b \simeq 0.5$.

We have calculated conditional and joint probabilities for a set of arbitrary points of space to remain in the false vacuum at different times, and for two points on a bubble wall or on two different bubble walls to remain uncollided. We have also considered the probability that a point on a wall is uncollided, in the presence of another bubble. It is straightforward to generalize these derivations to other cases, such as the probability that a point on a wall is uncollided assuming that a given point in space is in the false vacuum, or considering more than two points on bubble walls.

Our results can be directly applied to the calculation of some consequences of the phase transition, such as the generation of a stochastic background of gravitational waves. Different types of phase transitions can be considered by choosing different functions $\Gamma(t)$ and $v(t)$, and our results can be used to compare different models¹⁹. Our method can also be generalized to calculate the probability that a region of false vacuum has been trapped by several bubbles of true vacuum, which is crucial in the dynamics of defect formation. We shall address some of these applications elsewhere. Here, we have limited

¹⁹Some models were already considered in Ref. [44].

ourselves to discussing the behavior of some related quantities. To conclude, we summarize the general qualitative features of these quantities. For a given bubble, the functions $\langle S(t)S(t') \rangle$ and $\langle S(t) \rangle \langle S(t') \rangle$ are qualitatively and quantitatively similar. In particular, we have $\langle S^2(t) \rangle \simeq \langle S(t) \rangle^2$ at the beginning of the phase transition, the difference becoming important at later times. We also have $\langle S(t)S(t') \rangle \simeq \sqrt{\langle S^2(t) \rangle \langle S^2(t') \rangle}$, the difference becoming important only for large $|t' - t|$. On the other hand, for different bubbles, their surface correlation only becomes important when they are close to each other (i.e., when the separation l between their centers becomes close to the bubble diameter $2R$). On the other hand, on a given bubble surface, the correlation between points disappears in general when the points are separated by an angle $\theta \gtrsim \pi/2$.

Acknowledgments

This work was supported by CONICET grant PIP 11220130100172 and Universidad Nacional de Mar del Plata, grant EXA897/18.

A Bubble configurations for two point conditional probability

In this appendix we consider the two orderings of the times t_N, t'_N, t' which were not considered in Fig. 7.

The case $t'_N < t_N < t'$ is illustrated in Fig. 14 for some values of t'' . The configuration for $t'' > t'$ is not shown, since in this case the nucleation at t'' cannot affect the events at times t', t'_N or t_N , and we have

$$dP(t'') = dt'' \Gamma(t'') \frac{4\pi}{3} R(t'', t)^3 \quad (t'' > t'). \quad (72)$$

In the case $t_N < t'' < t'$ (left panel), a bubble nucleated at time t'' may have eaten the point p' at time t' , so we must exclude the striped region,

$$dP(t'') = dt'' \Gamma(t'') \left[\frac{4\pi}{3} R(t'', t)^3 - V_\cap \right] \quad (t'_N < t'' < t'). \quad (73)$$

For $t'_N < t'' < t_N$ (central panel), the nucleation at t'' may also prevent the nucleation of bubble B . Therefore, we must exclude the pink region as well as the striped region, and we have

$$dP(t'') = dt'' \Gamma(t'') \left[\frac{4\pi}{3} R(t'', t)^3 - \frac{4\pi}{3} R(t'', t_N)^3 - V_\cap + V'_\cap \right] \quad (t'_N < t'' < t_N). \quad (74)$$

Finally, for $t'' < t'_N$, (right panel), the nucleation at t'' may also prevent the nucleation of bubble B' , but the region which can affect this event (orange shade) is completely contained within the striped region, and we obtain again Eq. (74).

Now let us consider the case $t'_N < t' < t_N$, which is illustrated in Fig. 15. For $t'' > t'$, the bubble B' and the point p' cannot be affected by nucleations at t'' , and we have, for the case $t'' > t_N$ (not shown in the figure)

$$dP(t'') = dt'' \Gamma(t'') \frac{4\pi}{3} R(t'', t)^3 \quad (t'' > t_N), \quad (75)$$

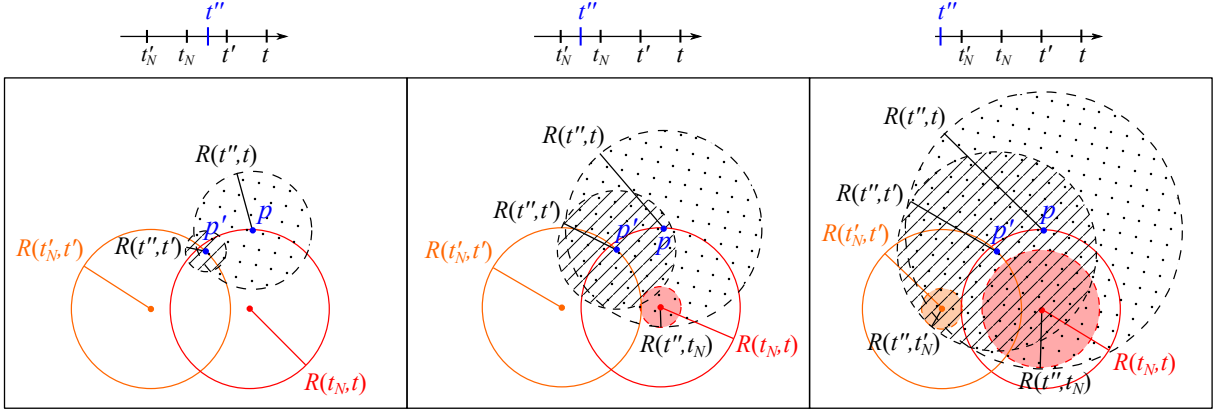


Figure 14: Like Fig. 7, for the time ordering $t'_N < t_N < t'$.

while for the case $t'' < t_N$ (left panel),

$$dP(t'') = dt'' \Gamma(t'') \frac{4\pi}{3} [R(t'', t)^3 - R(t'', t_N)^3] \quad (t' < t'' < t_N). \quad (76)$$

For $t'_N < t'' < t'$ (central panel), the point p' can be affected, and we have

$$dP(t'') = dt'' \Gamma(t'') \left[\frac{4\pi}{3} R(t'', t)^3 - \frac{4\pi}{3} R(t'', t_N)^3 - V_\cap + V'_\cap \right] \quad (t'_N < t'' < t'). \quad (77)$$

Finally, for $t'' < t'_N$ (right panel), the nucleation of B' can also be affected, but this is already taken into account in Eq. (77), since the orange region is always contained in the striped region.

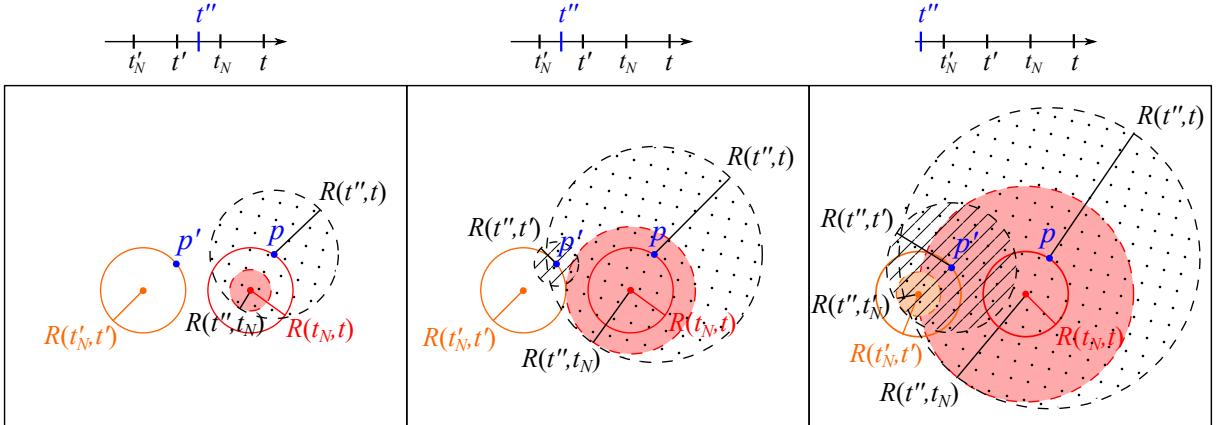


Figure 15: Like Fig. 7, for the time ordering $t'_N < t' < t_N$.

These results lead to Eqs. (42-43). In particular, Eqs. (73) and (77) show that the volume V_\cap appears for $t'' < t'$, as expressed by the upper limit of the integral (15), while Eqs. (74) and (77) show that the volume V'_\cap appears for $t'' < \min\{t_N, t'\}$, as expressed by the upper limit of the integral (43).

References

- [1] Michael S. Turner, Erick J. Weinberg, and Lawrence M. Widrow. Bubble nucleation in first order inflation and other cosmological phase transitions. *Phys. Rev.*, D46:2384–2403, 1992.
- [2] Marc Kamionkowski, Arthur Kosowsky, and Michael S. Turner. Gravitational radiation from first order phase transitions. *Phys. Rev. D*, 49:2837–2851, 1994.
- [3] Sidney R. Coleman. The Fate of the False Vacuum. 1. Semiclassical Theory. *Phys. Rev. D*, 15:2929–2936, 1977. [Erratum: *Phys.Rev.D* 16, 1248 (1977)].
- [4] Jr. Callan, Curtis G. and Sidney R. Coleman. The Fate of the False Vacuum. 2. First Quantum Corrections. *Phys. Rev. D*, 16:1762–1768, 1977.
- [5] Dietrich Bodeker and Guy D. Moore. Can electroweak bubble walls run away? *JCAP*, 05:009, 2009.
- [6] Dietrich Bodeker and Guy D. Moore. Electroweak Bubble Wall Speed Limit. *JCAP*, 05:025, 2017.
- [7] Andrei D. Linde. Fate of the False Vacuum at Finite Temperature: Theory and Applications. *Phys. Lett. B*, 100:37–40, 1981.
- [8] Andrei D. Linde. Decay of the False Vacuum at Finite Temperature. *Nucl. Phys. B*, 216:421, 1983. [Erratum: *Nucl.Phys.B* 223, 544 (1983)].
- [9] N. Turok. Electroweak bubbles: Nucleation and growth. *Phys. Rev. Lett.*, 68:1803–1806, 1992.
- [10] Guy D. Moore and Tomislav Prokopec. How fast can the wall move? A Study of the electroweak phase transition dynamics. *Phys. Rev. D*, 52:7182–7204, 1995.
- [11] Edward Witten. Cosmic Separation of Phases. *Phys. Rev. D*, 30:272–285, 1984.
- [12] M. Laine. Bubble growth as a detonation. *Phys. Rev. D*, 49:3847–3853, 1994.
- [13] J. Ignatius, K. Kajantie, H. Kurki-Suonio, and M. Laine. The growth of bubbles in cosmological phase transitions. *Phys. Rev. D*, 49:3854–3868, 1994.
- [14] Ariel Megevand and Santiago Ramirez. Bubble nucleation and growth in very strong cosmological phase transitions. *Nucl. Phys. B*, 919:74–109, 2017.
- [15] John Ellis, Marek Lewicki, and Jos Miguel No. On the Maximal Strength of a First-Order Electroweak Phase Transition and its Gravitational Wave Signal. *JCAP*, 04:003, 2019.
- [16] Ryusuke Jinno, Thomas Konstandin, and Masahiro Takimoto. Relativistic bubble collisions—a closer look. *JCAP*, 09:035, 2019.
- [17] V.A. Kuzmin, V.A. Rubakov, and M.E. Shaposhnikov. On the Anomalous Electroweak Baryon Number Nonconservation in the Early Universe. *Phys. Lett. B*, 155:36, 1985.

- [18] Andrew G. Cohen, D.B. Kaplan, and A.E. Nelson. Progress in electroweak baryogenesis. *Ann. Rev. Nucl. Part. Sci.*, 43:27–70, 1993.
- [19] Antonio Riotto and Mark Trodden. Recent progress in baryogenesis. *Ann. Rev. Nucl. Part. Sci.*, 49:35–75, 1999.
- [20] David E Morrissey and Michael J Ramsey-Musolf. Electroweak baryogenesis. *New Journal of Physics*, 14(12):125003, dec 2012.
- [21] Michael S. Turner and Frank Wilczek. Relic gravitational waves and extended inflation. *Phys. Rev. Lett.*, 65:3080–3083, 1990.
- [22] Chiara Caprini et al. Science with the space-based interferometer eLISA. II: Gravitational waves from cosmological phase transitions. *JCAP*, 04:001, 2016.
- [23] Chiara Caprini et al. Detecting gravitational waves from cosmological phase transitions with LISA: an update. *JCAP*, 03:024, 2020.
- [24] Arthur Kosowsky, Michael S. Turner, and Richard Watkins. Gravitational radiation from colliding vacuum bubbles. *Phys. Rev. D*, 45:4514–4535, 1992.
- [25] Mark Hindmarsh, Stephan J. Huber, Kari Rummukainen, and David J. Weir. Gravitational waves from the sound of a first order phase transition. *Phys. Rev. Lett.*, 112:041301, 2014.
- [26] Arthur Kosowsky and Michael S. Turner. Gravitational radiation from colliding vacuum bubbles: envelope approximation to many bubble collisions. *Phys. Rev.*, D47:4372–4391, 1993.
- [27] T W B Kibble. Topology of cosmic domains and strings. *Journal of Physics A: Mathematical and General*, 9(8):1387–1398, aug 1976.
- [28] T.W.B. Kibble and Alexander Vilenkin. Phase equilibration in bubble collisions. *Phys. Rev. D*, 52:679–688, 1995.
- [29] Julian Borrill, T.W.B. Kibble, Tanmay Vachaspati, and Alexander Vilenkin. Defect production in slow first order phase transitions. *Phys. Rev. D*, 52:1934–1943, 1995.
- [30] Chiara Caprini, Ruth Durrer, and Geraldine Servant. Gravitational wave generation from bubble collisions in first-order phase transitions: An analytic approach. *Phys. Rev.*, D77:124015, 2008.
- [31] Ryusuke Jinno and Masahiro Takimoto. Gravitational waves from bubble collisions: An analytic derivation. *Phys. Rev.*, D95(2):024009, 2017.
- [32] Alan H. Guth and S.H.H. Tye. Phase Transitions and Magnetic Monopole Production in the Very Early Universe. *Phys. Rev. Lett.*, 44:631, 1980. [Erratum: *Phys.Rev.Lett.* 44, 963 (1980)].
- [33] Paul Joseph Steinhardt. Relativistic Detonation Waves and Bubble Growth in False Vacuum Decay. *Phys. Rev. D*, 25:2074, 1982.

- [34] M. Gyulassy, K. Kajantie, H. Kurki-Suonio, and Larry D. McLerran. Deflagrations and Detonations as a Mechanism of Hadron Bubble Growth in Supercooled Quark Gluon Plasma. *Nucl. Phys. B*, 237:477–501, 1984.
- [35] H. Kurki-Suonio. Deflagration Bubbles in the Quark - Hadron Phase Transition. *Nucl. Phys. B*, 255:231–252, 1985.
- [36] H. Kurki-Suonio and M. Laine. Supersonic deflagrations in cosmological phase transitions. *Phys. Rev. D*, 51:5431–5437, 1995.
- [37] Andrew F. Heckler. The Effects of electroweak phase transition dynamics on baryogenesis and primordial nucleosynthesis. *Phys. Rev. D*, 51:405–428, 1995.
- [38] Leonardo Leitao, Ariel Megevand, and Alejandro D. Sanchez. Gravitational waves from the electroweak phase transition. *JCAP*, 1210:024, 2012.
- [39] B. Link. Deflagration instability in the quark - hadron phase transition. *Phys. Rev. Lett.*, 68:2425–2428, 1992.
- [40] Patrick Y. Huet, Keijo Kajantie, Robert G. Leigh, Bao-Hua Liu, and Larry D. McLerran. Hydrodynamic stability analysis of burning bubbles in electroweak theory and in QCD. *Phys. Rev.*, D48:2477–2492, 1993.
- [41] Ariel Megevand and Federico Agustin Membiela. Stability of cosmological deflagration fronts. *Phys. Rev.*, D89(10):103507, 2014.
- [42] Ariel Megevand and Francisco Astorga. Generation of baryon inhomogeneities in the electroweak phase transition. *Phys. Rev. D*, 71:023502, 2005.
- [43] Ariel Mégevand and Santiago Ramírez. Bubble nucleation and growth in slow cosmological phase transitions. *Nucl. Phys.*, B928:38–71, 2018.
- [44] Ryusuke Jinno, Sangjun Lee, Hyeonseok Seong, and Masahiro Takimoto. Gravitational waves from first-order phase transitions: Towards model separation by bubble nucleation rate. *JCAP*, 11:050, 2017.